In Search of Excited-State Proton Transfer in the Lumichrome Dimer in the Solid State: Theoretical and Experimental Approach

Ewa Sikorska,[†] Igor Khmelinskii,[‡] Maciej Kubicki,[§] Wiesław Prukała,[§] Marcin Hoffmann,[§,⊥] Isabel F. Machado,[#] Luis F. V. Ferreira,[#] Jerzy Karolczak,[£,||] David R. Worrall,[¶] Alina Krawczyk,[§] Małgorzata Insińska-Rak,[§] and Marek Sikorski*[,§]

Faculty of Commodity Science, Poznań University of Economics, al. Niepodległości 10, 60-967 Poznań, Poland, Universidade do Algarve, DQB, FCT, Campus de Gambelas, Faro 8005-139, Portugal, Faculty of Chemistry, A. Mickiewicz University, Grunwaldzka 6, 60-780 Poznań, Poland, BioInfoBank Institute, Limanowskiego 24A, 60-744 Poznań, Poland, Centro de Química-Física Molecular, Complexo Interdisciplinar, Instituto Superior Técnico, 1049-001 Lisbon, Portugal, Faculty of Physics, A. Mickiewicz University, Umultowska 85, 61-614 Poznań, Poland, Center for Ultrafast Laser Spectroscopy, A. Mickiewicz University, Umultowska 85, 61-614 Poznań, Poland, and Department of Chemistry, Loughborough University, Loughborough, Leicestershire LE11 3TU, U.K.

Received: January 4, 2006; In Final Form: February 20, 2006

Quantum chemical density functional theory (DFT) calculations and spectral data were employed to investigate the possibility of the excited-state double proton transfer (ESDPT) in lumichrome crystals. The calculations in a lumichrome dimer predict a transfer of a proton in the first excited state, leading to a cation−anion pair. The presently reported X-ray structure of 1,3-dimethyllumichrome and its complex solid-state luminescence indicate that also in this molecule intermolecular hydrogen bonds might be involved in the photophysics. The long-wavelength emission in lumichrome crystals peaked at 530 nm is attributed to excited-state proton transfer, whereas a wider emission band in methylated lumichrome derivatives peaked at 560 nm is attributed to ions formed upon photoexcitation of the crystals.

Introduction

Discovery of excited-state double proton transfer (ESDPT) in the 7-azaindole dimer[1] prompted very intensive studies of this reaction. Despite the substantial research effort, definite answers about the ESDPT mechanism in this system remain an issue of continuing controversy. Indeed, previous studies showed that the ESDPT reaction occurs in 7-azaindole dimer that has a planar double hydrogen-bonded structure. The two well-known models of the ESDPT reaction in the 7-azaindole dimer differ in assuming either the concerted or the stepwise mechanism. Some of the very recent developments on the ESDPT reaction in the 7-azaindole dimer in the gas phase can be found in a series of papers by Sekiya and co-workers that contribute information on the evidence of complete localization in the lowest excited electronic state of asymmetric isotopomers,[2] the cooperative nature of double proton transfer revealed by H/D kinetic isotopic effects,[3] and on the reaction mechanism studied by picosecond time-resolved resonance-enhanced multiphoton ionization (REMPI) spectroscopy.[4] However, regardless of these recent developments the mechanism of ESDPT remains controversial, having revealed its complexity, especially in solution. The mechanism and kinetics of the ESDPT in the 7-azaindole dimer is being intensively studied by several groups;[5−15] for a review of the literature see, for example, refs 16−18 and references therein. The phenomenon of ESDPT is in no way limited to the 7-azaindole dimers. Following the initial studies of 7-azaindole, a number of other host/guest excited-state proton-transfer reactions have been studied. Some of the examples include hydroxyquinolines, carbazoles, indoles, β-carbolines, and other molecules in which the excited-state proton-transfer tautomerism is mediated by adding guest molecules, including solvent, upon forming host/guest hydrogen-bonded complexes; see, for example, ref 16 and references therein. Among the molecules studied was lumichrome = 7,8-dimethylalloxazine = 7,8-dimethyl-benzo[*g*]pteridine-2,4(1*H*,3*H*)-dione (see Figure 1), a representative of alloxazines (benzo[*g*]pteridine-2,4-(1*H*,3*H*)-diones). Acetic acid is of special interest as a guest molecule. The use of acetic acid as a proton-transfer agent is

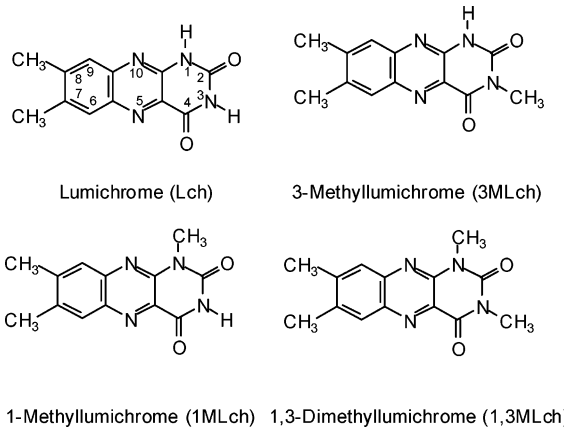

Figure 1. Structures of lumichrome, 1-methyllumichrome, 3-methyllumichrome, and 1,3-dimethyllumichrome.

* Corresponding author. Phone: +48 61 8291309. Fax: +48 61 8658008. E-Mail: sikorski@amu.edu.pl.
[†] Poznań University of Economics.
[‡] Universidade do Algarve.
[§] Faculty of Chemistry, A. Mickiewicz University.
[⊥] BioInfoBank Institute.
[#] Instituto Superior Técnico.
[£] Faculty of Physics, A. Mickiewicz University.
[||] Center for Ultrafast Laser Spectroscopy, A. Mickiewicz University.
[¶] Loughborough University.

10.1021/jp060072y CCC: $33.50
Published on Web 03/22/2006

particularly justified as its molecular structure remains unchanged upon the ESDPT process in, e.g., the acetic acid−lumichrome complex. Therefore, acetic acid serves as a simple yet powerful catalyst for the ESDPT.[19] On the other hand, the ESDPT reaction in the 7-azaindole dimer changes the structure of both molecules. As a result, the ESDPT reaction in 7-azaindole is a noncatalytic process in which the 7-azaindole dimer acts as a reactant rather than as a catalyst.

For a number of reasons it is interesting to look for the ESDPT reaction in the solid state. The ESDPT reaction does not occur in 7-azaindole crystals because of the absence of the dual hydrogen-bonded structure.[20] Thus, a wide search has been undertaken for other model systems that would allow us to investigate ESDPT reaction in crystals, although there exist only a very few experimental studies of ESDPT in systems other than the 7-azaindole dimer. The previously investigated systems include, for example, 3-methyl-7-azaindole,[20] 3-iodo-7-azaindole,[21] and 1-azacarbazole.[22]

In lumichrome there are several centers (oxygen atoms, nitrogen atoms, N−H groups), which may serve as hydrogen acceptors or hydrogen donors in the creation of hydrogen-bonded complexes. It was shown that proton-transfer reactions in lumichrome occur in the excited state. In this process the proton from the N(1) nitrogen atom of the lumichrome molecule is transferred to the N(10) nitrogen atom, and the excited isoalloxazinic form is created. It was shown that excited-state isomerization takes place in lumichrome and other N(1)-unsubstituted alloxazines in the presence of compounds having proton donor and acceptor functions and being able to form hydrogen bonds of appropriate strength and conformation with the alloxazinic molecules, i.e., acetic acid. Considerable work has been done to study the mechanism of the excited-state proton-transfer reaction in the lumichrome−acetic acid and other complexes.[23−38] Despite the early discovery and the number of reported studies, there are no reports about the ESDPT reaction in the lumichrome dimer. Our recently reported crystallographic data[23] prompted us to study the possible ESDPT reaction in this system.

The present paper describes a steady-state and time-resolved study on the ESDPT reaction in polycrystals of lumichrome and its 1- and 3-methyl and 1,3-dimethyl derivatives. We also report quantum mechanical calculations that shed new light on the mechanism of the ESDPT reaction in the lumichrome dimer system. Herein, we compare experimental and theoretical approaches to the ground- and excited-state double proton transfer reaction in the lumichrome dimer. The present theoretical investigation aims at providing a more systematic insight into the problem of the concerted versus the stepwise mechanism. The structures and abbreviations of the lumichromes discussed here are presented in Figure 1.

Experimental Section

Materials. Lumichrome, ethanol, and acetic acid from Aldrich were used as received. The 1-methyl-, 3-methyl-, and 1,3-dimethyllumichrome derivatives were available from previous work.

Spectral and Photophysical Measurements. All fluorescence lifetime measurements were performed in the front-face arrangement at the Centre for Ultrafast Laser Spectroscopy in Poznañ, using excitation at 380 nm. The fluorescence lifetime spectrophotometer, using the single-photon timing technique, has been described in detail elsewhere.[39] On the excitation side a Spectra-Physics picosecond/femtosecond laser system was used as the source of exciting pulses. A Tsunami Ti:sapphire laser, pumped with a BeamLok 2060 argon ion laser, tuneable in the 720−1000 nm range, generated 1−2 ps pulses at a repetition rate of about 82 MHz and average power of over 1 W. The repetition rate ranged from 4 MHz to single shot using a model 3980-2S pulse selector. Second and third harmonics of the picosecond pulse obtained on a GWU-23PS harmonic generator could be used for excitation, giving great flexibility in the choice of the excitation wavelength. Elements of an Edinburgh Instruments FL900 system were used in the optical and control units of the system. The pulse timing and data-processing systems employed a biased TAC model TC 864 (Tenelec) and the R3809U-05 MCP-PMT emission detector with thermoelectric cooling and appropriate preamplifiers (Hamamatsu). Steady-state fluorescence spectra were obtained on a Jobin Yvon-Spex Fluorolog 3-11 spectrofluorometer, and UV−vis absorption spectra were obtained on a Varian Cary 5E spectrophotometer. Unless otherwise indicated, the samples were in equilibrium with air. All measurements were performed at room temperature.

Laser-induced fluorescence (LIF) emission measurements of the samples were performed at room temperature in the front-face arrangement in Lisbon. A detailed description together with a diagram of the system has been presented in ref 40. Briefly, as the excitation source the system uses the 337.1 nm pulse of a N_2 laser (Photon Technology Instruments, model 2000, ca. 600 ps fwhm, ∼1.3 mJ/pulse). At the detection side a gated intensified charge-coupled device (ICCD, Oriel model Instaspec V) is used to collect light arising from the samples. The ICCD is coupled to a fixed compact imaging spectrograph (Oriel, model FICS 77441). The system can be used either by capturing all light emitted by the sample or in the time-resolved mode by using a delay generator (Stanford Research Systems, model DG535) with a suitable gate width. The ICCD has high-speed (2.2 ns) gating electronics and covers the 200−900 nm wavelength range. Time-resolved absorption and emission spectra are available in the nanosecond to second time range.[40−42]

Quantum Mechanical Calculations. Information on the electronic structure and geometry of the lumichrome dimer was obtained with the use of quantum chemical density functional theory (DFT) calculations. The calculations were performed using the B3LYP functional[43] in conjunction with a split-valence 6-31G(d†) polarized basis set.[44] Full optimization of the geometrical parameters of the complex of the two reacting molecules at this level of theory produced three ground-state potential energy minima. Transition states connecting these minima were also found, and intrinsic reaction coordinate (IRC) calculations followed by full geometry optimization (pseudo-IRC) verified that the obtained transition states indeed connect these three energy minima. The vertical excitation energies and oscillator strengths were computed using the time-dependent (TD) approach as implemented in the Gaussian 03 program.[45] Predicted lowest-energy singlet−singlet transitions of lumichromes, $S_0 \rightarrow S_i$, were calculated for the ground-state geometry. The excitation energies computed using the TD-B3LYP/6-31G(d†) level of theory are estimated to be accurate within 2000−3000 cm^{-1}, usually requiring a shift toward the red to reproduce experimental spectra. However, regarding the quality of our spectral predictions it should be noted that the difference in the experimental transition energies in 1,4-dioxane solution between lumiflavin and lumichrome (22.7 and 26.4 × 10^3 cm^{-1}) is reproduced in the calculations (24.5 and 27.8 × 10^3 cm^{-1}) to within 0.5 × 10^3 cm^{-1},[46] with the predicted values blue-shifted as compared to the experimental ones by less than 2.0 × 10^3 cm^{-1}.

TABLE 1: Crystal Structure and Structure Refinement Parameters of 1,3-Dimethyllumichrome[a]

empirical formula	$C_{14}H_{14}N_4O_2$	
formula weight	270.29	
temperature	293(2) K	
wavelength	0.71073 Å	
crystal system	triclinic	
space group	P$\bar{1}$	
unit-cell dimensions	$a = 7.7387(13)$ Å	$\alpha = 106.152(15)°$
	$b = 13.090(2)$ Å	$\beta = 89.790(14)°$
	$c = 13.141(2)$ Å	$\gamma = 92.074(13)°$
volume	1277.8(3) Å^3	
Z	4	
density (calcd)	1.405 mg/m^3	
absorption coefficient	0.098 mm^{-1}	
$F(000)$	568	
θ range for data collection	3.04−22.50°	
index ranges	$-8 \le h \le 5$	
	$-13 \le k \le 14$	
	$-14 \le l \le 13$	
reflections collected	5445	
independent reflections	3252 [R(int) = 0.0591]	
completeness to $\theta = 22.50°$	97.3%	
refinement method	full-matrix least-squares on F^2	
data/restraints/parameters	3252/0/369	
goodness of fit on F^2	1.059	
final R indices [$I > 2\sigma(I)$]	R1 = 0.0937, wR2 = 0.1763	
R indices (all data)	R1 = 0.1812, wR2 = 0.2166	
largest diff. peak and hole	0.186 and −0.245 e·Å^{-3}	

[a] Crystallographic data, tables of atomic coordinates, thermal parameters, bond lengths, and bond angles have been deposited with the Cambridge Crystallographic Data Centre, CCDC, with the deposition no. CCDC 290325. Copies of this information may be obtained free of charge from the Director, CCDC, 12 Union Road, Cambridge CB2 1EZ, U.K. (Fax: +44 1223 336 033. E-mail: deposit@ccdc.cam.ac.uk or http://www.ccdc.cam.ac.uk.)

To gain insight into geometry relaxation of the first excited state, geometry optimization at the TD-B3LYP/6-31(d†) level was carried out. These were extremely lengthy calculations, in which the Gaussian03 program was used to calculate energies, and numerical gradients of energy were obtained in a "shamefully" parallel way, whereby single-point energies were used to obtain numerical gradients via a simple perl code. Then TINKER code[47−50] was then used to calculate an optimization step. The whole procedure was repeated until a geometry change of at least 0.001 Å was unable to improve the system energy.

X-ray Crystal Structural Analysis. A colorless 0.1 × 0.3 × 0.4 mm^3 crystal was chosen for X-ray data collection. Diffraction data were collected at 100(1) K by the ω-scan technique up to $2\theta = 60°$, on a KUMA-KM4CCD diffractometer [Oxford Diffraction (2003), CrysAlisCCD, User Guide v.171, Oxford Diffraction Poland Sp., Wrocław, Poland] with graphite-monochromatized Mo Kα radiation ($\lambda = 0.71073$ Å). The data were corrected for Lorentz-polarization effects [Oxford Diffraction (2003), CrysAlisRed, CCD data reduction GUI v.171, Oxford Diffraction Poland Sp., Wrocław, Poland]. Accurate unit-cell parameters were determined by a least-squares fit of 3943 reflections of highest intensity, chosen from the whole experiment. The structure was solved with SHELXS97[51] and refined with the full-matrix least-squares procedure on F^2 by SHELXL97.[52] Scattering factors incorporated in SHELXL97 were used. The function $\sum w(|F_o|^2 - |F_c|^2)^2$ was minimized, with $w^{-1} = [\sigma^2(F_o)^2 + 0.0841P^2]$, where P is [Max $(F_o^2, 0) + 2F_c^2$]/3. All non-hydrogen atoms were refined anisotropically; hydrogen atoms were located in subsequent difference Fourier maps, and their positional and isotropic displacement parameters were refined. The relevant crystal data are listed in Table 1, together with the refinement details.

Results and Discussion

X-ray Analysis. Only a limited amount of crystallographic data is available for lumichromes. For example, only recently we reported crystallographic data for unsubstituted lumichrome.[23] Very briefly, crystallographic data indicate that the lumichrome molecules are arranged into dimers in the crystal structure by means of intermolecular hydrogen bonds.[23] As we reported recently, the N1−H1···N10($-x$, $1 - y$, $2 - z$) hydrogen bonds connect molecules into centrosymmetric dimers, additionally strengthened by C9−H9···O2($-x$, $1 - y$, $2 - z$) hydrogen bonds. These dimers are further connected with other dimers by pairs of centrosymmetric N3−H3···O4($1 - x$, $1 - y$, $1 - z$) hydrogen bonds. The tapes of molecules are stacked one onto another with the interplanar distance of ca. 3.25 Å. Presently we succeeded in obtaining crystallographic data of 1,3-dimethyllumichrome; however, the crystal structures of 1-methyllumichrome and 3-methyllumichrome remain unknown. Crystallographic data of 1,3-dimethyllumichrome are summarized in Table 1. The asymmetric part of the unit cell contains two symmetry-independent molecules (referred to as **A** and **B**) of 1,3-dimethyllumichrome. The normal probability plot[53,54] shows that the differences in the molecular geometry are statistical rather than systematic (correlation coefficient is 0.97). The perspective view of the molecule **A** is shown in Figure 2. The

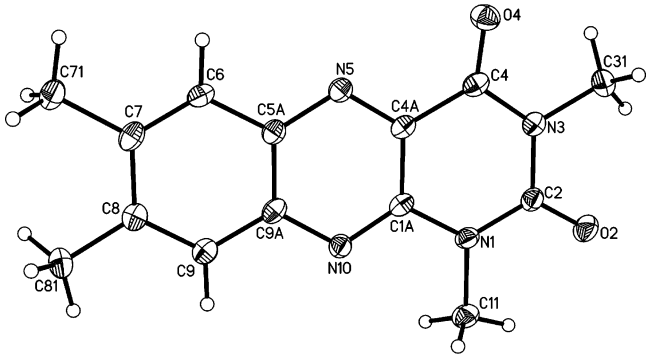

Figure 2. Anisotropic-ellipsoid representation of **1A**, together with the numbering scheme. The ellipsoids are drawn at the 50% probability level; hydrogen atoms are represented by spheres of arbitrary radii.

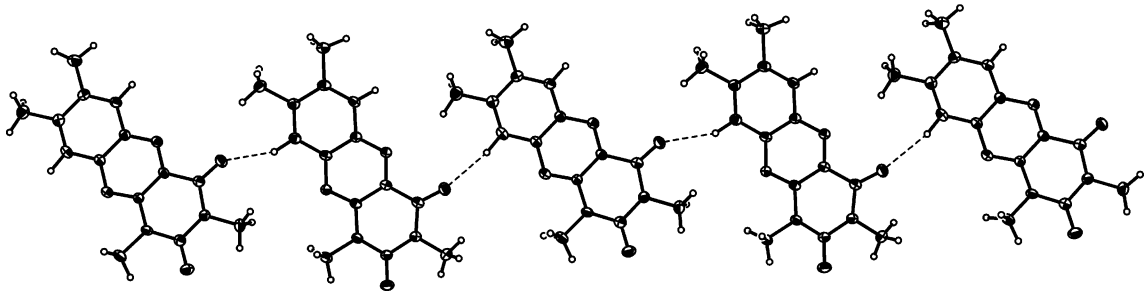

Figure 3. C−H···O hydrogen-bonded chain (∼**ABAB**∼ sequence) of the molecules of **1**. The chain extends along the [−111] direction; hydrogen bonds are depicted as dashed lines.

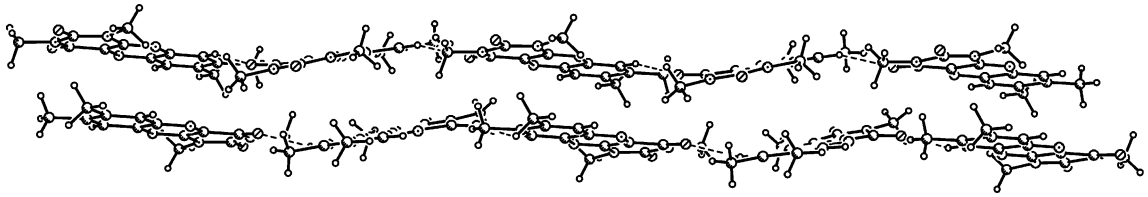

Figure 4. Overlap of molecules of the neighboring chains, connected by a center of inversion. Hydrogen bonds are depicted as dashed lines; the distance between the average planes of the molecules is close to 2.3 Å.

bond lengths and angles are quite typical, both molecules being almost planar: the maximum deviation from the least-squares plane calculated for all 14 ring atoms is equal to 0.093(2) Å in molecule **A** and 0.068(2) Å in molecule **B**. The dihedral angles between constituent rings are also small (note that the deviations from planarity are only significant for ring A)—the angles between the planes of the terminal rings are 3.5(1)° and 2.5-(1)° for molecules **A** and **B**.

The crystal packing is determined—besides the van der Waals interactions—by relatively strong C9−H9···O4 hydrogen bonds (H···O contact is 2.31(2) Å) that connect molecules into infinite ∼**ABABAB**∼ chains along the [−111] direction (Figure 3). These chains are connected into centrosymmetric pairs (Figure 4); the cohesion between the chains is probably provided by significant $\pi-\pi$ interactions: the distances between the average planes of molecules **A** and **B** are shorter than 3.3 Å. This interaction connects similar molecules, i.e., **A**−**A** and **B**−**B**. Additionally, pairs of chains are connected by means of a (dipole−dipole)-type interaction between the C═O double bonds of molecules **A** and **B**. Allen et al.[55] have shown that such interactions can successfully compete with hydrogen bonds in certain circumstances; in the present case the C···O distance is quite short (3.029(3) and 2.974(3) Å), and the O···O distance is even shorter (2.866(2) Å). The C═O···C angles are not far from 90°, they are equal to 105.8(2)° and 108.8(2)°; thus, this interaction is close to the "perpendicular motif", using Allen's nomenclature.[55]

Spectroscopic and Photophysical Properties. A typical fluorescence of lumichrome in acetonitrile presented in Figure 5 exhibits a maximum at about 437 nm, to be compared with that of lumichrome polycrystals. The excitation was performed at 355 nm in both experiments. The spectrum of polycrystals may be further compared to that of lumichrome in acetonitrile with acetic acid and to that of lumiflavin, a molecule of isoalloxazinic structure. The fluorescence maximum shifts to longer wavelengths (530 nm) in the two cases when lumichrome can interact with the acetic acid and also in the spectrum of lumiflavin. The emission spectra of polycrystalline samples of lumichrome, much different from the corresponding spectra of lumichrome adsorbed into microcrystalline cellulose and, especially, from those in solutions, lead us to believe that crystalline lumichrome and other alloxazine derivatives exhibit emission originating from their respective dimers.[56−58]

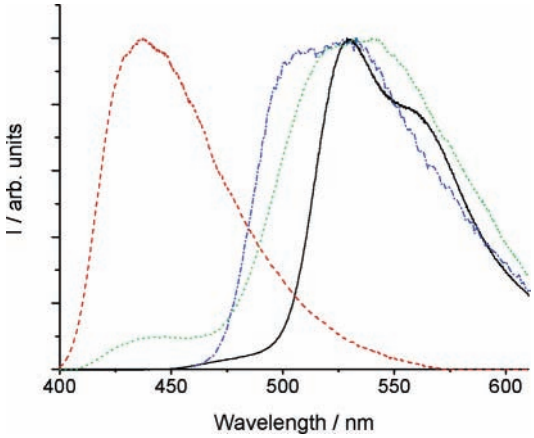

Figure 5. Normalized fluorescence emission spectra of lumichrome polycrystals (solid line), lumichrome with (green dotted line) and without acetic acid (red dashed line), and lumiflavin (blue dash−dotted line), all in acetonitrile.

Our hypothesis was based on the fact that their crystal structures admit the possibility of ESDPT, provided there exists a center of symmetry at the geometric center of the planar arrangement of four nitrogen atoms N(10), N(1), N′(10), N′(1) belonging to two adjacent molecules (see Scheme 2 from ref 58). Our very recent X-ray diffraction results[23] showed that hydrogen bonds play an essential role in the formation of the lumichrome crystal structure and indeed lead to dimer formation, which is allowed by symmetry. These findings lead us to the necessity of a more detailed study of crystal solids of lumichrome and its derivatives, as possible candidates for the ESDPT reaction.

First, we shall review the behavior of lumichrome and its derivatives in solution and especially the ESDPT reaction of lumichrome in the presence of acetic acid. In a number of previous studies we have reported spectroscopic and photophysical properties of lumichrome, its 1- and 3-methyl and 1,3-dimethyl derivatives, and other alloxazines in different solvents.[24,37,46,59−63] The absorption spectrum of lumichromes in solution exhibits two low-energy absorption bands. The absorption spectra of lumichrome and its presently studied derivatives are essentially identical, which makes them a very interesting set of structurally related compounds to be used in studies of

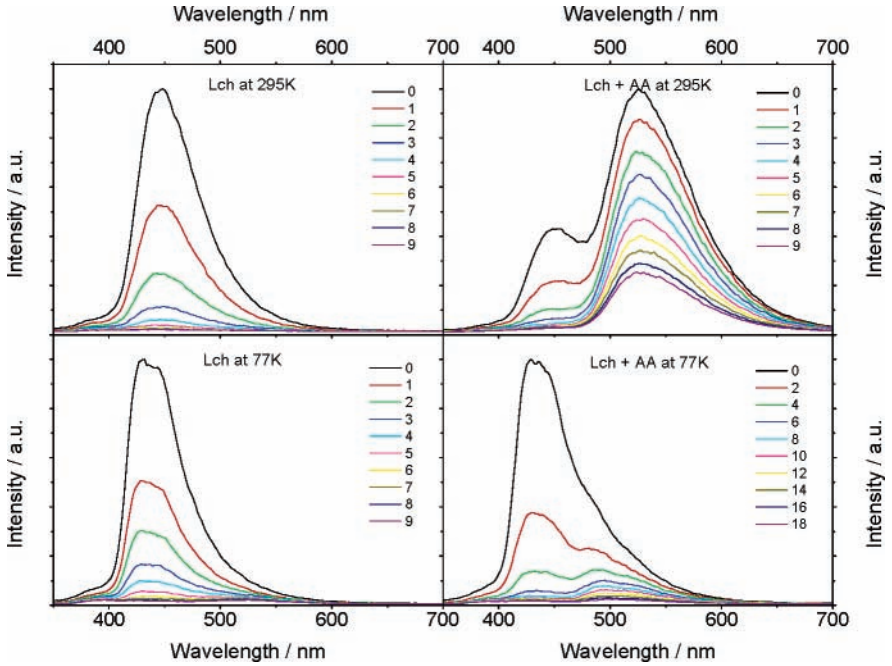

Figure 6. Time-resolved fluorescence spectra of lumichrome: in ethanol at room temperature (Lch at 298 K), at room temperature with 2.79 mol dm^{-3} of acetic acid (Lch + AA at 298 K), in ethanol at 77 K (Lch at 77 K), and in ethanol with 2.79 mol dm^{-3} of acetic acid at 77 K (Lch + AA at 77 K). Excitation was at 337 nm in all samples; the spectra were recorded with the time delays (ns) indicated on the respective panel.

the ESDPT reaction in host/guest systems. Two of the compounds, lumichrome and 3-methyllumichrome, selectively allow ESDPT involving proton transfer from N(1) to N(10). On the contrary, two other compounds, 1-methyl- and 1,3-dimethyllumichrome, selectively prohibit such a proton-transfer reaction. In addition, the methyl group in position 3 (3-methyllumichrome and 1,3-methyllumichrome) makes the respective nitrogen atom structurally uncreative. It is also to be mentioned that 5-deazalumichrome, also available for study, had been reported to be active in ESDPT.[25] The two strong longer-wavelength absorption bands of lumichrome and its methyl-substituted derivatives, with their maxima at about 336 and 385 nm in solution, have been assigned to two independent π,π^* transitions.[34,59] However, as is the case of many aza-aromatics, each of these lowest-energy π,π^* transitions is accompanied by a closely lying n,π^* transition; experimentally, they overlap and show up as a single broad band. These conclusions were supported by polarization spectroscopy results obtained by Sun et al.[34] and by us.[64] In conformity, our recent theoretical studies predict that the transitions observed in all of these lumichromes are of the π,π^* character. The two calculated lowest-energy π,π^* transitions are located at approximately 316 and 359 nm (31.7×10^3 and 27.8×10^3 cm^{-1}) and are accompanied by two closely located n,π^* transitions at 313 and 362 nm (31.9×10^3 and 27.6×10^3 cm^{-1}) of low oscillator strength. The weak fluorescence emission of alloxazines, relative to that of isoalloxazines, results from the close spacing between the n,π^* and π,π^* singlet excited states.

The fluorescence emission spectra of lumichrome and its derivatives in solutions show a single band with the maximum at about 448 nm (see Figures 5 and 6). To help establish the role of the N(1)−H and N(3)−H groups in the proton-transfer reaction, model compounds 1-methyllumichrome and 1,3-dimethyllumichrome were employed.[63] The methyl group at N(1) and/or N(3) allows the effect of the lumichrome−acetic acid interaction to be selectively observed. A new longer-wavelength emission band appears for lumichrome and 3-methyllumichrome in the presence of acetic acid, whereas no such band is observed for either 1-methyllumichrome or 1,3-dimethyllumichrome. The new emission observed for a 3-methyl- and lumichrome with a maximum at about 527 nm is similar to the emission spectrum of the compounds with isoalloxazinic structure (e.g., lumiflavin or riboflavin in solutions) and has been identified as emission of the isoalloxazinic form appearing as a result of excited-state proton transfer from N(1) to N(10). The intensity of alloxazinic emission at about 446 nm decreased, and the intensity of isoalloxazinic emission at about 527 nm increased, with increasing acetic acid concentration.[63] As an example, we have recorded time-resolved fluorescence spectra of lumichrome in the nanosecond time range in ethanol at room temperature with 2.79 mol dm^{-3} of acetic acid and without acetic acid, see Figure 6. Lumichrome and its methyl-substituted derivatives in ethanol without acetic acid show a single fluorescence maximum at about 445 nm; the spectra are almost identical for all of the samples and in general closely reproduce the steady-state fluorescence spectra. The time evolution of the fluorescence spectra suggests that the fluorescence lifetimes are virtually constant throughout the spectrum, remaining in the nanosecond time range. Temperature change from 289 to 77 K does not affect significantly either the emission spectrum or kinetics of lumichrome (see the two left panels in Figure 6). However, apart from alloxazinic emission at 445 nm, a new isoalloxazinic band at about 530 nm appears in the time-resolved fluorescence emission spectra of lumichrome in ethanol in the presence of 2.79 mol dm^{-3} of acetic acid, excited at 337 nm. This new long-wavelength emission has a much longer fluorescence lifetime if compared to that of alloxazinic emission at shorter wavelengths. The new isoalloxazinic emission in solution is only present for lumichrome and 3-methyl-lumichrome. On the other hand, for 1-methyl-lumichrome and 1,3-dimethyllumichrome the time evolution of the fluorescence spectra indicates that only alloxazinic emission is present, with the fluorescence lifetime remaining largely unaffected by the presence of acetic acid. Interestingly, lowering the temperature for a sample of lumichrome in the presence of acetic acid the long-wavelength emission almost vanishes at 77 K; this can be

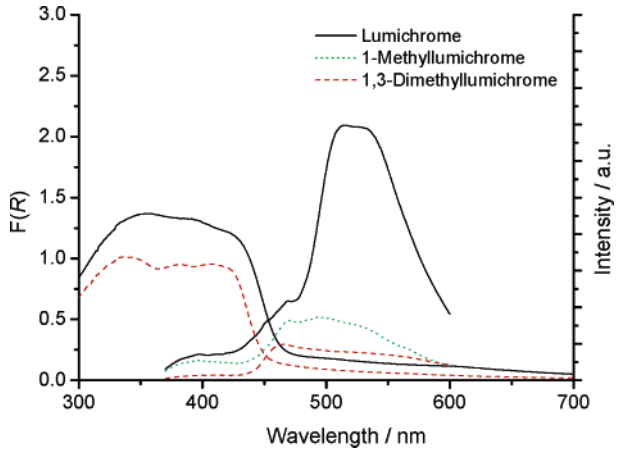

Figure 7. Ground-state diffuse reflectance absorption spectra of lumichrome and 1,3-dimethyllumichrome polycrystals plotted using the Kubelka−Munk remission function together with the fluorescence emission spectra. Luminescence spectra of lumichrome, 1-methyllumichrome, and 1,3-dimethyllumichrome polycrystals excited at 355 nm are shown.

explained on the basis of the activation barrier for the ESDPT reaction, which had been estimated to be about 7.8 kcal/mol in the first excited state.[63]

Ground-state diffuse reflectance absorption spectra of lumichrome and its 1- and 3-methyl and 1,3-dimethyl derivatives in the polycrystalline state were recorded and plotted in Figure 7 in terms of the Kubelka−Munk remission function, $F(R)$. $F(R)$ is proportional to the absorber concentration and is defined in the Kubelka−Munk theory of the interaction of light with opaque materials as

$$F(R) = (1 - R)^2/2R = K/S \qquad (1)$$

where R represents the observed diffuse reflectance from the sample surface, K and S are absorption and scattering coefficients, respectively, both measured in (distance)$^{-1}$ units and wavelength-dependent.[65,66]

The spectral bands are interpreted by comparison to those of the respective solution spectra. In general, the absorption edge is shifted to the red in solid crystals as compared to solutions. However, there are a number of reasons to believe that the situation in solids is more complicated than that in solutions, especially intriguing being the cases of 1-methyllumichrome and 1,3-dimethyllumichrome, which should not participate in the ESDPT if we adopt that same logic that works in solutions and inhibits the ESDPT between the acetic acid and the 1-substituted lumichromes. Diffuse reflectance absorption spectra show some differences between lumichrome and 1,3-dimethyllumichrome, probably caused by strong interactions being present in lumichrome. In this respect, let us consider the luminescence spectra recorded for lumichrome, 1-methyllumichrome, and 1,3-dimethyllumichrome presented in Figure 7. These luminescence spectra look much different if compared to the respective spectra in solutions. We note at least three distinct regions in the lumichrome luminescence spectrum, with the corresponding maxima at about 400, 470, and 520 nm, the last being the most intense. The luminescence intensities of 1-methyllumichrome and 1,3-dimethyllumichrome are much lower, and in the steady-state spectra show no peak around 520 nm, with some other differences also present. For example, in 1,3-dimethyllumichrome the short-wavelength emission at 400 nm is almost absent, while the luminescence of 1-methyllumichrome and lumichrome in the same region is very similar. It should be noted that the overall emission from 1,3-dimethyllumichrome is significantly lower than that from the other two derivatives, and the 400 nm emission will be strongly reabsorbed by the ground state. The emission at about 470 nm is present in all three derivatives; however, since this appears on the falling edge of the absorption band, there may be some influence of the reabsorption and reemission distorting the spectrum and hence shifting the observed maximum to longer wavelength. Additionally, 1-methyllumichrome shows an emission maximum around 490 nm, which is absent in 1,3-dimethyllumichrome. It has to be noted that luminescence quantum yields and band maxima are basically identical for all of these lumichromes in solutions; however, quantitative comparisons of emission intensities in the solid state are difficult. In the case of lumichrome, the emission at 530 nm could have its origins in the same phenomenon as observed in solution, i.e., excited-state proton transfer in the solid state, since crystal structure data confirm that strong interactions are possible. In the case of 1-methyllumichrome, the 530 nm emission is much reduced or absent as expected, and the long-wavelength emission must have its origins in a phenomenon other than proton transfer.[23,24,38,63] As shown in the next section, the observed emission band can be resolved into separate contributions through time-resolved emission measurements. Thus, because of the complex crystal structure and possible interactions, some other type of lumichrome emission has to be considered. Indeed, emission from different types of cationic and anionic forms of lumichromes had been reported earlier in solutions, in separate experiments, usually shifted respectively to the blue and to the red, compared to the neutral form.[67] Additionally, emission from a simple dimer without proton-transfer interactions cannot be discounted; a red-shifted broad emission in, for example, anthracene has been assigned as excimer fluorescence[68] and has been observed in crystals, low-temperature glasses, and from aggregates on the surface of silica gel.[69]

In some respect our expectations that using a set of lumichromes with and without a methyl group at position 1 and/or 3 would help in a straightforward discussion of the ESDPT reaction in solid lumichrome were less justified if compared to the ESDPT reaction in solutions. Taking into account that lumichromes are capable of forming various hydrogen bonds because of a number of active centers at N(10), N(5), N(3), and N(1), and at both carbonyl oxygen atoms, it is reasonable to expect a more complex situation in the crystal solids. Introduction of a methyl group, apart from affecting the possibility of the ESDPT reaction, necessarily changes the crystal packing and alters the role of specific intermolecular interactions, such as those with participation of carbonyl oxygen atoms; some of these interactions would still be effective even in 1-methyl- and 1,3-dimethyllumichrome. For now, strong interactions in solid crystals together with an appropriate geometric arrangement of molecules can be seen as a working hypothesis that explains the presence of different types of emission in lumichromes including the long-wavelength emission observed in 1-methyl- and 1,3-dimethyllumichrome, to be discussed next. These results suggest the importance of molecular interactions in the crystal packing of lumichromes in the solid state, as evident from our X-ray data for lumichrome[23] and 1,3-dimethyllumichrome (the structure of 1,3-dimethyllumichrome was discussed above). Clearly, further work is needed to clarify the crystal packing in 1-methyllumichrome and 3-methyllumichrome. Until now, all of our attempts to obtain suitable crystals of these two compounds have failed; nevertheless, the

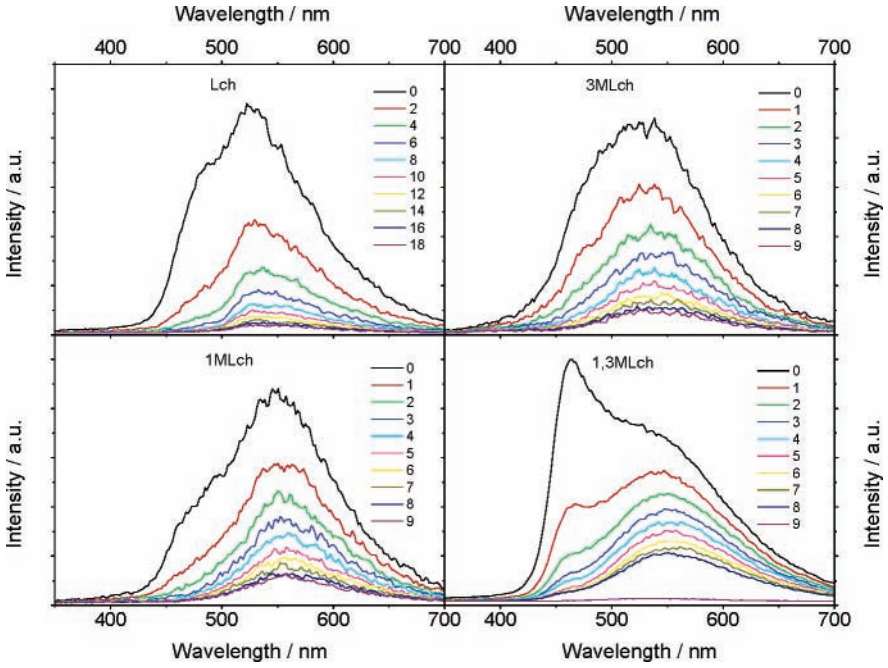

Figure 8. Time-resolved fluorescence spectra of polycrystalline samples of lumichrome, 1-methyl-lumichrome, 3-methyl-lumichrome, and 1,3-dimethyl-lumichrome. Excitation was at 337 nm for all of the samples; the spectra were recorded with the time delays (ns) indicated on the respective panel.

relatively strong hydrogen bonds determining the crystal packing are also expected to operate in these two remaining lumichromes.

To study the effect of the crystal packing on the photophysical properties, we recorded time-resolved luminescence emission spectra of polycrystals of lumichrome and its 1- and 3-methyl and 1,3-dimethyl derivatives. The emission was excited at 337 nm, with the results presented in Figure 8. These results indicate that for all of the lumichrome polycrystals, a new long-wavelength emission is observed. As evident from the steady-state spectra, the intensities of these long-wavelength emissions are much reduced in the derivatives relative to those of the parent lumichrome and are only observed through time-resolved emission measurements. Additionally, the longer-wavelength emission in the derivatives peaks at 560 nm, instead of 530 nm in the parent lumichrome, with the respective band being significantly wider. Thus, there is an important difference between the results in solutions and in solid crystals: in the latter, weak long-wavelength emission is observed even for 1-methyllumichrome and 1,3-dimethyllumichrome. As can be seen from Figure 8, the band at longer wavelengths in all cases has a much longer fluorescence lifetime if compared to that of alloxazinic emission at shorter wavelengths. Note, however, the special spectral shape of the fluorescence observed for 1,3-dimethyllumichrome, indicating that the longer-wavelength emission is much weaker if compared to that of other lumichromes studied and, thus, most probably has a source different from that of unsubstituted lumichrome polycrystals.

Another important difference between solutions and polycrystals becomes obvious when we compare room-temperature results of lumichrome to those obtained at 77 K, see Figure 9. The temperature strongly affects the intensity ratio between normal and tautomeric emission in ethanolic solutions of lumichrome with acetic acid, indicating that the excited-state process is less efficient at lower temperatures. In polycrystalline samples, however, the temperature affects the intensity ratio only very weakly if at all, with the longer-wavelength emission remaining dominant even at low temperatures. These results

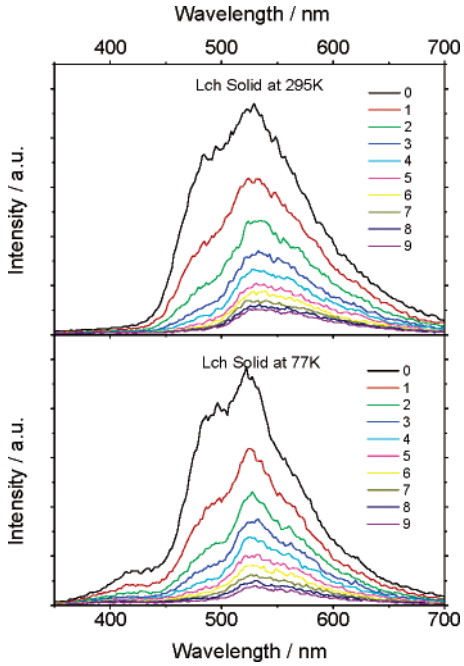

Figure 9. Time-resolved fluorescence spectra of lumichrome polycrystals at room temperature (top panel) and at 77 K (bottom panel). Excitation was at 337 nm; the spectra were recorded with the time step of 1 ns.

demonstrate that the activation barrier for the respective process in crystals is significantly lower than that in solutions.

Once again, in analogy to the previous studies in solutions, we employed single-photon timing technique to measure the emission lifetimes quantitatively and to learn more about the excited-state dynamics in crystals. The lumichrome emission decays were recorded at different wavelengths: 480, 530 (not shown), and 600 nm. Typical decay curves are shown in Figure 10. The usage of several wavelengths allowed us to obtain clear spectral separation of the two types of emission, which can be problematic to recognize for nonexperts in the time-resolved

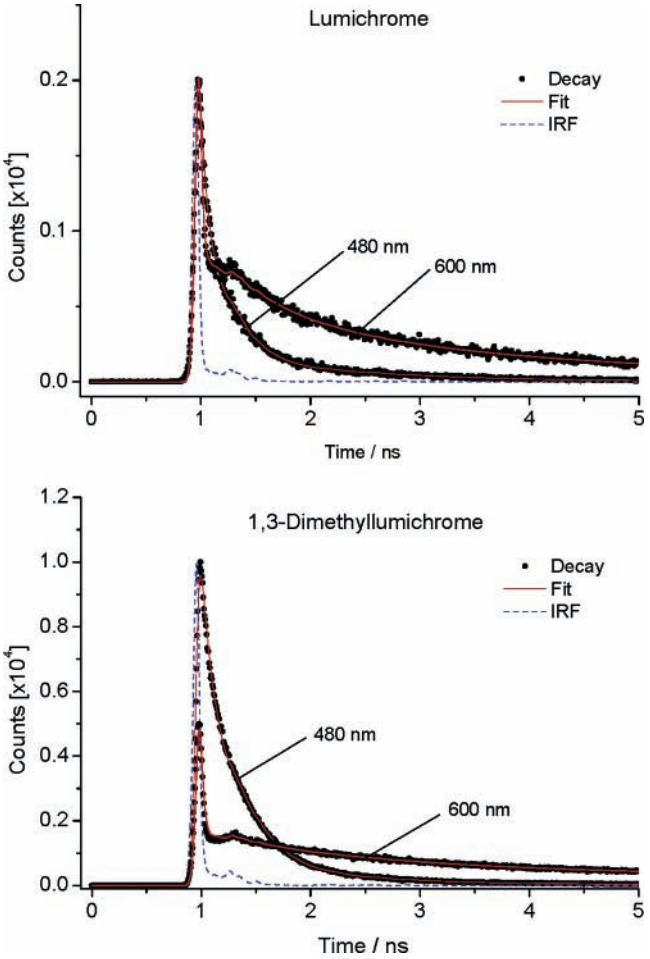

Figure 10. Typical fluorescence decays of polycrystalline samples. Top panel: lumichrome, observed at 480 nm and fitted with a biexponential function $\tau_{F1} = 0.24$ ns, $\tau_{F2} = 1.35$ ns, $\chi^2 = 1.2$; and lumichrome, observed at 600 nm and fitted with a biexponential function $\tau_{F1} = 0.64$ ns, $\tau_{F2} = 3.26$ ns, $\chi^2 = 1.2$. Bottom panel: 1,3-dimethyllumichrome, observed at 480 nm and fitted with a biexponential function $\tau_{F1} = 0.32$ ns, $\tau_{F2} = 1.71$ ns, $\chi^2 = 1.2$; and 1,3-dimethyllumichrome, observed at 600 nm and fitted with a biexponential function $\tau_{F1} = 1.21$ ns, $\tau_{F2} = 7.23$ ns, $\chi^2 = 1.2$.

fluorescence spectra. We should note that, contrary to the results in solutions, no rise time is observed in solid crystals, as the reaction is predicted to be very fast—with very low activation energy if any—and the dimer of lumichrome has the correct geometry for the reaction to occur.

The biexponential fits are not perfect; however, we should note that the measurements of solid polycrystalline samples present certain difficulties, to mention only the presence of strong scattered light, heterogeneous nature of the sample, its porous structure, and problems with the response function. However, the biexponential fits provide a rationale for seeking a mechanism in which at least two distinct emitting species exist. Note that the shorter-lived component has a lifetime shorter or about 1 ns, whereas the longer-lived component has in most cases a lifetime longer than 1 ns. Since these ranges of the lifetimes are not too different from those registered when the alloxazines and isoalloxazines are separately excited in solutions, it might be tempting to assign the shorter-lived component to the neutral excited alloxazinic species and the longer-lived component to a separate excited species, perhaps formed as the result of the ESDPT reaction, anion form of lumichrome in singlet excited state, or strongly hydrogen-bond interacting molecule. Therefore, to clarify the situation we will limit the following discussion based on the calculations to the unsubstituted lumichrome dimer.

TABLE 2: Selected Geometrical Parameters for the Potential Energy Minima and Transition States in the Ground and the First Excited State of the Lumichrome Dimer

	A	**AB**	**B**	**BC**	**C**	**AC**	**B_{exc}**
ΔE [kcal/mol]	0.0	20.3	20.0	23.5	10.8	25.9	41.2
d1 [Å]	1.087	1.083	1.083	1.080	1.088	1.082	1.083
d2 [Å]	2.137	2.036	2.051	1.896	2.050	1.860	2.158
d3 [Å]	3.223	3.109	3.124	2.960	3.128	2.927	3.231
d4 [Å]	1.027	1.060	1.065	1.283	1.977	1.351	1.021
d5 [Å]	2.143	1.803	1.820	1.411	1.040	1.303	2.172
d6 [Å]	3.170	2.863	2.885	2.694	3.016	2.654	3.191
d7 [Å]	2.143	1.208	1.116	1.084	1.040	1.303	1.017
d8 [Å]	1.027	1.508	1.668	1.685	1.977	1.351	2.286
d9 [Å]	3.170	2.717	2.783	2.768	3.016	2.654	3.293
d10 [Å]	1.087	1.087	1.090	1.088	1.088	1.082	1.090
d11 [Å]	2.137	1.808	1.829	1.890	2.050	1.860	2.560
d12 [Å]	3.223	2.887	2.913	2.966	3.128	2.927	3.631
a1 [°]	177.58	170.59	170.40	167.61	170.50	167.99	170.56
a2 [°]	179.17	177.48	178.39	179.26	176.18	177.86	175.55
a3 [°]	179.17	179.09	178.12	175.25	176.18	177.86	170.26
a4 [°]	177.58	171.53	171.99	169.09	170.50	167.99	167.29

Calculated Ground-State Proton Transfer in the Lumichrome Dimer. Table 2 presents selected geometrical parameters of the potential energy minima and the transition states for the lumichrome dimer, as predicted in our calculations. The initial structure **A**, in which d7 = 2.143 and d8 = 1.027 Å, undergoes the reaction leading to a cation−anion structure **B** (see Figure 11).

In structure **B**, which corresponds to a very shallow potential energy minimum, one of the two lumichrome molecules transfers its proton, thus becoming an anion, to the other lumichrome molecule that becomes a cation. For structure **B** d7 = 1.116 and d8 = 1.668 Å. The transition state **AB**, whose relative (to that of the initial structure **A**) energy is 20.3 kcal/mol, closely resembles structure **B**—the d7 and d8 distances are 1.208 and 1.508 Å, respectively. The very shallow minimum **B** has the relative energy of 20.0 kcal/mol—only 0.3 kcal/mol below the energy of the transition state **AB** (see Figure 12).

The transfer of the second proton from the cationic form present in structure **B** to the anionic form leads to the formation of structure **C**. The relative energy of the transition state **BC** is 23.5 kcal/mol, while for structure **C** it is 10.8 kcal/mol. The geometry changes corresponding to the imaginary frequency in the **AB** and **BC** transition states are presented in the Supporting Information to this paper as animations. The distances that change the most during this reaction step are d4 and d5. They are 1.065 and 1.820 Å in **B**, 1.283 and 1.411 Å in **BC**, and 1.977 and 1.040 Å in **C**. Attempts to obtain a transition state that connects structures **A** and **C** directly proved partially successful when symmetry constraints were imposed. However, the energy of the transition state **AC** was higher than that for the transition state **BC** (25.9 kcal/mol). Moreover, vibrational analysis indicated that structure **AC** is in fact a second-order saddle point and not a transition state, as two vibrations with imaginary frequencies were identified.

Calculated Excited-State Proton Transfer in the Lumichrome Dimer. Vertical excitation energies calculated for the ground-state potential energy minima are 3.35, 1.58, and 2.98 eV for structures **A**, **B**, and **C**, respectively (see Figure 13). Interestingly, a scan of the energy hypersurface of the first excited state along the ground-state reaction coordinate indicated that there is only one excited-state potential energy minimum

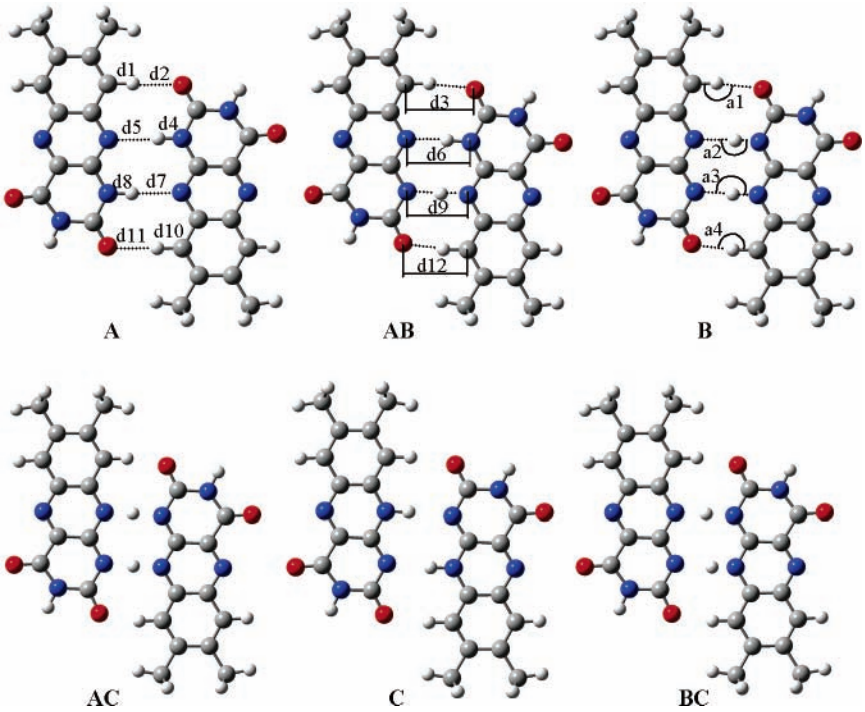

Figure 11. Ground-state minima and transition states connecting various tautomeric forms of the lumichrome dimer.

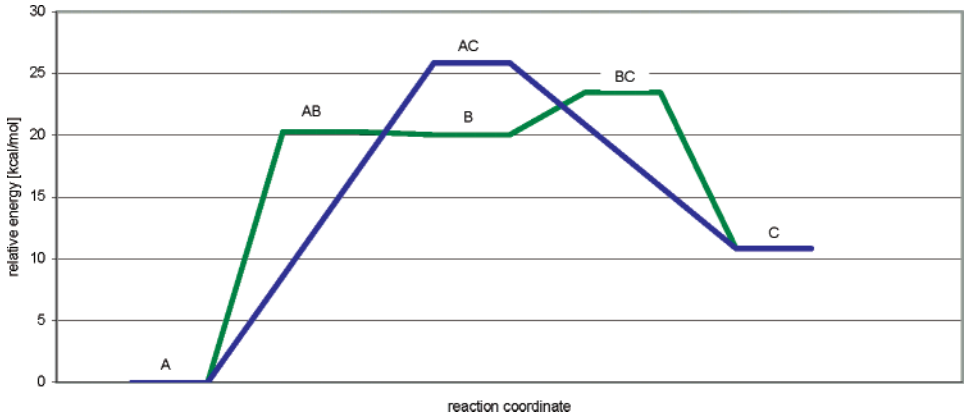

Figure 12. Relative energies of the potential energy minima and transition states for the ground-state proton-transfer reaction in the lumichrome dimer.

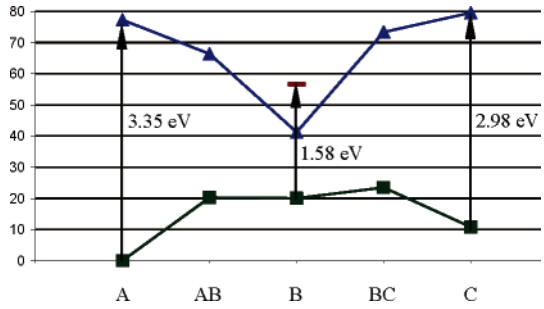

Figure 13. Potential energy hypersurfaces of the ground and first excited state. There are three potential energy minima in the ground state but only one in the first excited state, in which the cation−anion pair is present. The energies of vertical excitations from the ground-state minima are shown as arrows.

corresponding to the structure **B**, as there is no energy barrier for a transition from **A** to **B** and from **C** to **B**. Indeed, tedious optimization of the first excited-state geometry starting from the ground-state geometry of structure **A** leads to a structure of a dimer where the cation−anion pair is present. This structure corresponds to the **B** structure, with some minor differences in geometric parameters. The separation between cation and anion is larger for the first excited-state minimum $\mathbf{B}_{exc}$ than for the ground-state structure **B**. For the $\mathbf{B}_{exc}$ structure the distances between the nitrogen atoms from the two lumichrome molecules involved in the hydrogen bonds are 3.191 and 3.293 Å for distances d6 and d9, respectively. In the case of structure **B** these distances are 2.885 and 2.783 Å. In parallel, the proton acceptor distances of these hydrogen bonds are 2.172 and 2.286 Å for distances d5 and d8 in structure $\mathbf{B}_{exc}$ and 1.820 and 1.668 Å in structure **B**.

Excited-State Proton Transfer in Crystals. Quantum mechanical calculations indicate that three minima, corresponding to different arrangements of NH protons in the lumichrome dimer, may exist in the ground state. The process of proton transfer in the lumichrome dimer seems to be stepwise: first an NH proton is transferred from one lumichrome molecule to the other, forming a cation−anion pair, and then another NH proton is transferred from the protonated cation to the anion forming a pair of tautomeric forms of lumichrome. The activation barrier for the whole process of double proton transfer is relatively high, about 23.5 kcal/mol. It should be mentioned

that the minimum for the cation−anion pair is very shallow—only 0.3 kcal/mol is needed to overcome the energy barrier leading back to the initial lumichrome dimer. Therefore, this state may become a shoulder at the potential energy hypersurface at a more advanced computational level of theory. However, the situation is very different in the first excited state. Only a single potential energy minimum is observed—the one in which the cation−anion lumichrome pair is formed. Therefore, theoretical calculations seem to indicate that the excitation of lumichrome in its dimer results in a barrier less NH proton transfer from one lumichrome molecule to the other and formation of the cation−anion pair. However, in the ground state the cation−anion pair needs only a very small energy—0.3 kcal/mol (significantly less than its thermal energy of ca. 0.9 kcal/mol at room temperature) to converge to the initial lumichrome dimer.

Acknowledgment. Interdisciplinary Grant No. 51103-504 from the A. Mickiewicz University and the University of Economics, Poznañ, Poland, to M.S. and E.S., is gratefully acknowledged. The fluorescence lifetime measurements were performed at the Center for Ultrafast Laser Spectroscopy, Adam Mickiewicz University, Poznañ, Poland. All of the calculations were performed at the Poznañ Supercomputing and Networking Centre (PCSS).

Supporting Information Available: Movies showing the geometry changes corresponding to the imaginary frequency in the **AB** and **BC** transition states. This material is available free of charge via the Internet at http://pubs.acs.org.

References and Notes

(1) Taylor, C. A.; El-Bayoumi, M. A.; Kasha, M. *Proc. Natl. Acad. Sci. U.S.A* **1969**, *63*, 253.
(2) Sakota, K.; Sekiya, H. *J. Phys. Chem. A* **2005**, *109*, 2718.
(3) Sakota, K.; Sekiya, H. *J. Phys. Chem. A* **2005**, *109*, 2722.
(4) Sakota, K.; Okabe, C.; Nishi, N.; Sekiya, H. *J. Phys. Chem. A* **2005**, *109*, 5245.
(5) Catalan, J.; De Paz, J. L. G. *J. Chem. Phys.* **2005**, *122*, art-244320.
(6) Catalan, J.; Perez, P.; Del Valle, J. C.; De Paz, J. L. G.; Kasha, M. *Proc. Natl. Acad. Sci. U.S.A.* **2004**, *101*, 419.
(7) Sakai, M.; Fujii, M. *Chem. Phys. Lett.* **2004**, *396*, 298.
(8) Catalan, J.; Perez, P.; Del Valle, J. C.; De Paz, J. L. G.; Kasha, M. *Proc. Natl. Acad. Sci. U.S.A.* **2002**, *99*, 5799.
(9) Catalan, J. *J. Phys. Chem. A* **2002**, *106*, 6738.
(10) Sakai, M.; Ishiuchi, S.; Fujii, M. *Eur. Phys. J. D* **2002**, *20*, 399.
(11) Folmer, D. E.; Wisniewski, E. S.; Castleman, A. W. *Chem. Phys. Lett.* **2000**, *318*, 637.
(12) Takeuchi, S.; Tahara, T. *Chem. Phys. Lett.* **1997**, *277*, 340.
(13) Chou, P. T.; Wei, C. Y.; Chang, C. P.; Kuo, M. S. *J. Phys. Chem.* **1995**, *99*, 11994.
(14) Douhal, A.; Kim, S. K.; Zewail, A. H. *Nature* **1995**, *378*, 260.
(15) Share, P.; Pereira, M.; Sarisky, M.; Repinec, S.; Hochstrasser, R. M. *J. Lumin.* **1991**, *48*−*9*, 204.
(16) Waluk, J. *Conformational Analysis of Molecules in Excited States*; Wiley-VCH: New York, 2000.
(17) Agmon, N. *J. Phys. Chem. A* **2005**, *109*, 13.
(18) Dermota, T. E.; Zhong, Q.; Castleman, A. W. *Chem. Rev.* **2004**, *104*, 1861.
(19) Chou, P. T.; Wei, C. Y.; Chang, C. P.; Chiu, C. H. *J. Am. Chem. Soc.* **1995**, *117*, 7259.
(20) Yu, W. S.; Cheng, C. C.; Chang, C. P.; Wu, G. R.; Hsu, C. H.; Chou, P. T. *J. Phys. Chem. A* **2002**, *106*, 8006.
(21) Chou, P. T.; Liao, J. H.; Wei, C. Y.; Yang, C. Y.; Yu, W. S.; Chou, Y. H. *J. Am. Chem. Soc.* **2000**, *122*, 986.
(22) Waluk, J.; Herbich, J.; Oelkrug, D.; Uhl, S. *J. Phys. Chem.* **1986**, *90*, 3866.
(23) Sikorska, E.; Khmelinskii, I. V.; Kubicki, M.; Prukala, W.; Nowacka, G.; Siemiarczuk, A.; Koput, J.; Ferreira, L. F. V.; Sikorski, M. *J. Phys. Chem. A* **2005**, *109*, 1785.
(24) Sikorska, E.; Koziolowa, A.; Sikorski, M.; Siemiarczuk, A. *J. Photochem. Photobiol. A* **2003**, *157*, 5.
(25) Koziolowa, A.; Visser, N. V.; Koziol, J.; Szafran, M. M. *J. Photochem. Photobiol., A* **1996**, *93*, 157.
(26) Zen, Y. H.; Wang, C. M. *J. Chem. Soc., Chem. Commun.* **1994**, 2625.
(27) Tyrakowska, B.; Koziolowa, A.; Bastiaens, P. I. H.; Visser, A. J. W. G. *Flavins Flavoproteins, Proc. Int. Symp.* **1991**, *10*, 45.
(28) MacInnis, J. M.; Kasha, M. *Chem. Phys. Lett.* **1988**, *151*, 375.
(29) Koziolowa, A.; Visser, A. J. W. G.; Koziol, J. *Photochem. Photobiol.* **1988**, *48*, 7.
(30) Song, P. S.; Choi, J. D. *Bull. Korean Chem. Soc.* **1980**, *1*, 93.
(31) Choi, J. D.; Fugate, R. D.; Song, P. S. *J. Am. Chem. Soc.* **1980**, *102*, 5293.
(32) Fugate, R. D.; Song, P. S. *Photochem. Photobiol.* **1976**, *24*, 479.
(33) Song, P. S.; Sun, M.; Koziolowa, A.; Koziol, J. *J. Am. Chem. Soc.* **1974**, *96*, 4319.
(34) Sun, M.; Moore, T. A.; Song, P. S. *J. Am. Chem. Soc.* **1972**, *94*, 1730.
(35) Kasha, M. *J. Chem. Soc., Faraday Trans. 2* **1986**, *82*, 2379.
(36) Heelis, P. F.; Koziolowa, A. *J. Photochem. Photobiol., B* **1991**, *11*, 365.
(37) Sikorska, E.; Szymusiak, H.; Khmelinskii, I. V.; Koziolowa, A.; Spanget-Larsen, J.; Sikorski, M. *J. Photochem. Photobiol., A* **2003**, *158*, 45.
(38) Sikorska, E.; Koziolowa, A. *J. Photochem. Photobiol., A* **1996**, *95*, 215.
(39) Karolczak, J.; Komar, D.; Kubicki, J.; Wrozowa, T.; Dobek, K.; Ciesielska, B.; Maciejewski, A. *Chem. Phys. Lett.* **2001**, *344*, 154.
(40) Botelho do Rego, A. M.; Ferreira, L. F. V. Photonic and Electronic Spectroscopies for the Characterization of Organic Surfaces and Organic Molecules Adsorbed on Surfaces. In *Handbook of Surfaces and Interfaces of Materials*; Nalwa, H. S., Ed.; Academic Press: New York, 2001; Vol. 2, Chapter 7.
(41) Ferreira, L. F. V.; Machado, I. F.; Da Silva, J. P.; Oliveira, A. S. *Photochem. Photobiol. Sci.* **2004**, *3*, 174.
(42) Ferreira, L. F. V.; Machado, I. F.; Oliveira, A. S.; Ferreira, M. R. V.; Da Silva, J. P.; Moreira, J. C. *J. Phys. Chem. B* **2002**, *106*, 12584.
(43) Becke, A. D. *J. Chem. Phys.* **1993**, *98*, 5648.
(44) Ditchfield, R.; Hehre, W. J.; Pople, J. A. *J. Chem. Phys.* **1971**, *54*, 724.
(45) Frisch, M. J.; Trucks, G. W.; Schlegel, H. B.; Scuseria, G. E.; Robb, M. A.; Cheeseman, J. R.; Zakrzewski, V. G.; Montgomery, A. J., Jr.; Stratmann, R. E.; Burant, J. C.; Dapprich, S.; Millam, J. M.; Daniels, A. D.; Kudin, K. N.; Strain, M. C.; Farkas, O.; Tomasi, J.; Barone, V.; Cossi, M.; Cammi, R.; Mennucci, B.; Pomelli, C.; Adamo, C.; Clifford, S.; Ochterski, J.; Petersson, G. A.; Ayala, P. Y.; Cui, Q.; Morokuma, K.; Malick, D. K.; Rabuck, A. D.; Raghavachari, K.; Foresman, J. B.; Cioslowski, J.; Ortiz, J. V.; Stefanov, B. B.; Liu, G.; Liashenko, A.; Piskorz, P.; Komaromi, I.; Gomperts, R.; Martin, R. L.; Fox, D. J.; Keith, T.; Al-Laham, M. A.; Peng, C. Y.; Nanayakkara, A.; Gonzalez, C.; Challacombe, M.; Gill, P. M. W.; Johnson, B.; Chen, W.; Wong, M. W.; Andres, J. L.; Gonzalez, C.; Head-Gordon, M.; Replogle, E. S.; Pople, J. A. *Gaussian 98*, revision A.11.3.; Gaussian, Inc.: Pittsburgh, PA, 2002.
(46) Sikorska, E.; Khmelinskii, I. V.; Prukala, W.; Williams, S. L.; Patel, M.; Worrall, D. R.; Bourdelande, J. L.; Koput, J.; Sikorski, M. *J. Phys. Chem. A* **2004**, *108*, 1501.
(47) Ren, P. Y.; Ponder, J. W. *J. Phys. Chem. B* **2003**, *107*, 5933.
(48) Ren, P. Y.; Ponder, J. W. *J. Comput. Chem.* **2002**, *23*, 1497.
(49) Pappu, R. V.; Hart, R. K.; Ponder, J. W. *J. Phys. Chem. B* **1998**, *102*, 9725.
(50) Hodsdon, M. E.; Ponder, J. W.; Cistola, D. P. *J. Mol. Biol.* **1996**, *264*, 585.
(51) Sheldrick, G. M. *Acta Crystallogr., Sect. A* **1990**, *46*, 467.
(52) Sheldrick, G. M. *SHELXL-97, Program for the Refinement of Crystal Structure*; University of Gottingen: Gottingen, Germany, 1997.
(53) Abrahams, S. C.; Keve, E. T. *Acta Crystallogr., Sect. A* **1971**, *25*, 157.
(54) *International Tables for X-ray Crystallography*; Kluwer: Dordrecht, The Netherlands, 1974; p 293.
(55) Allen, F. H.; Baalham, C. A.; Lommerse, J. P. M.; Raithby, P. R. *Acta Crystallogr., Sect. B* **1998**, *54*, 320.
(56) Sikorski, M. *Determination of Spectroscopic and Photophysical Properties of Some Substances in Turbid or Other Non-Transmissive Media*; A. Mickiewicz University Press: Poznan, 2002; pp 1−143.
(57) Sikorski, M.; Sikorska, E.; Wilkinson, F.; Steer, R. P. *Can. J. Chem.* **1999**, *77*, 472.
(58) Mir, M.; Sikorska, E.; Sikorski, M.; Wilkinson, F. *J. Chem. Soc., Perkin Trans. 2* **1997**, 1095.
(59) Koziolowa, A. *Photochem. Photobiol.* **1979**, *29*, 459.

(60) Koziolowa, A.; Szymusiak, H.; Koziol, J. *Pol. J. Chem.* **1993**, *67*, 1813.
(61) Sikorska, E.; Khmelinskii, I. V.; Bourdelande, J. L.; Bednarek, A.; Williams, S. L.; Patel, M.; Worrall, D. R.; Koput, J.; Sikorski, M. *Chem. Phys.* **2004**, *301*, 95.
(62) Sikorska, E.; Khmelinskii, I. V.; Williams, S. L.; Worrall, D. R.; Herance, R. J.; Bourdelande, J. L.; Koput, J.; Sikorski, M. *J. Mol. Struct.* **2004**, *697*, 199.
(63) Sikorska, E.; Khmelinskii, I. V.; Hoffmann, M.; Machado, I. F.; Ferreira, L. F. V.; Dobek, K.; Karolczak, J.; Krawczyk, A.; Insinska-Rak, M.; Sikorski, M. *J. Phys. Chem. A* **2005**, *109*, 11707.
(64) Sikorska, E.; Koziolowa, A. *Studies in Commodity Science and Chemistry* **1993**, *Z. 210*, 79.
(65) Wilkinson, F.; Kelly, G. Diffuse Reflectance Flash Photolysis. In *Handbook of Organic Photochemistry*; Scaiano, J. C., Ed.; CRC Press: Boca Raton, FL, 1989.
(66) Kubelka, P.; Munk, F. *Z. Tech. Phys.* **1931**, *12*, 593.
(67) Lasser, N.; Feitelson, J. *Photochem. Photobiol.* **1977**, *27*, 451.
(68) Hoshino, M.; Seki, H.; Imamura, M.; Yamamoto, S. *Chem. Phys. Lett.* **1984**, *104*, 369.
(69) Wilkinson, F.; Worrall, D. R.; Williams, S. L. *J. Phys. Chem.* **1995**, *99*, 6689.